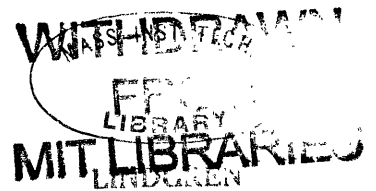


THE ACOUSTICAL TRANSMISSION RESPONSE OF  
AN OCEAN BOTTOM SEDIMENTARY LAYER

by  
Warren D. Moon



Submitted in Partial Fulfillment  
of the Requirements for the  
Degree of Master of Science  
at the  
Massachusetts Institute of Technology

June 1966

Signature of Author .....  
Department of Geology and Geophysics May 20, 1966

Certified by .....  
Thesis Supervisor

Accepted by .....  
Chairman, Departmental Committee on Theses

To my Father and Mother

TABLE OF CONTENTS

	<u>Page</u>
List of Illustrations.....	ii
Preface.....	iii
Abstract.....	v
1.0 INTRODUCTION.....	1
2.0 THEORETICS	
2.1 Physical Model and Notation.....	4
2.2 Electroacoustic Transducers.....	4
2.2.1 Sound Source.....	4
2.2.2 Receiver.....	6
2.3 Mathematical Models	
2.3.1 Reflection and Transmission at Interfaces.....	7
2.3.2 Spreading Loss.....	9
2.3.3 Attenuation.....	11
2.3.4 Energy Spectrums of Seismic Reflections.....	12
2.3.5 Transmission Response of First Sedimentary Layer.....	16
3.0 EMPIRICS	
3.1 Original Data.....	18
3.2 Signal Processing.....	19
3.3 Results.....	23
3.3.1 Oscillograms of the Seismic Returns.....	23
3.3.2 Energy Spectrums of the Seismic Reflections.....	31
3.3.3 Attenuation in the Sedimentary Layer.....	35
4.0 CONCLUSIONS.....	39
5.0 RECOMMENDED FUTURE INVESTIGATION.....	43
References.....	45

LIST OF ILLUSTRATIONS

	<u>Page</u>
Figure 1. GEOMETRY AND NOTATION FOR PHYSICAL MODEL.....	5
Figure 2. PRESSURE WAVE FROM A SPARKER.....	7
Figure 3. SPREADING LOSS GEOMETRY.....	10
Figure 4. MULTIPLE SOUND ARRIVAL PATHS.....	13
Figure 5. SEISMIC REFLECTION PROFILE IN AN AREA OF THE RED SEA.....	20
Figure 6. SURFACE WAVE AND SEISMIC REFLECTIONS FROM BOTTOM AND SUB-BOTTOM.....	25
Figure 7. BOTTOM AND TWO SUB-BOTTOM SEISMIC REFLECTIONS.....	26
Figure 8. BOTTOM AND FIRST SUB-BOTTOM SEISMIC REFLECTIONS.....	26
Figure 9. SEISMIC RETURN WITH HIGH-PASS FILTERING.....	27
Figure 10. SEISMIC RETURN WITH BAND-PASS FILTERING.....	28
Figure 11. SEISMIC RETURN WITH HIGH-PASS FILTERING.....	30
Figure 12. ENERGY SPECTRUMS OF BOTTOM AND SUB-BOTTOM SEISMIC REFLECTIONS #1.....	32
Figure 13. ENERGY SPECTRUMS OF BOTTOM AND SUB-BOTTOM SEISMIC REFLECTIONS #2.....	33
Figure 14. ACOUSTICAL TRANSMISSION RESPONSE OF FIRST SEDIMENTARY LAYER AS CALCULATED FROM TWO DIFFERENT SEISMIC RETURNS.....	36
Figure 15. ACOUSTICAL TRANSMISSION RESPONSE OF FIRST SEDIMENTARY LAYER AS CALCULATED FROM TWO DIFFERENT SEISMIC RETURNS.....	38

## PREFACE

The ocean is one of the great frontiers awaiting man's inevitable advance. Knowledge of the geology beneath the ocean's floor is indispensable to such things as the search and extraction of fossil fuels and minerals; the construction of marine civil engineering projects; modern warfare where, for example, submarines may make use of navigational systems relying on geological phenomena, and submarine commanders must know where they can safely rest their vessels on the ocean's floor; and scientific investigations of many kinds. Additionally, in a regenerative learning process, knowledge of sub-marine geology is important to the development of instrumentation and techniques for use in gaining more and better knowledge of the same kind.

In the spirit of helping to meet the above indicated need, this monograph presents work which was aimed at the development of a new approach to the study of the acoustical properties of sediments below the ocean's bottom. One of the goals was to investigate the possibility of recognizing the kinds of sediments through interrogation with sound initiated and received from a ship on the ocean's surface. Another goal was to investigate the possibility of acoustical interrogation as a means of determining certain properties of sediments, irrespective of the types of sediments which are important to the needs indicated in the above paragraph. For example, Whitman<sup>1</sup> has treated the problem of large structures in certain geological

---

<sup>1</sup>Superscript numbers will hereinafter refer to the references at the end of this monograph.

mediums developing resonant frequencies in the audio range.

\* \* \* \* \*

I wish to express my especial appreciation to three gentlemen whose help was so important to this research: to Dr. J. B. Hersey of the Woods Hole Oceanographic Institution for his excellent guidance and technical advice as my thesis advisor, to Dr. H. E. Edgerton of the Massachusetts Institute of Technology for kindly allowing me to use his laboratory facilities and supplies, and to Dr. H. J. Woll of the Radio Corporation of America for his generous provision of computer programming assistance and time on the RCA 301 Computer.

ABSTRACT

Detailed spectral analyses of seismic reflections from the ocean's bottom and first sub-bottom sedimentary interfaces were performed for each of two returns recorded during seismic reflection profiling. By this means, the acoustical transmission response of the first sub-bottom sedimentary layer was determined. The surprising results showed that the in situ oceanic sedimentary layer exhibited an acoustic attenuation in the 75 to 600 cps frequency range which varied up and down in magnitude. This is in contrast to the expected steadily increasing attenuation with increasing frequency.

Tentative hypotheses explaining these results are presented. The results of this investigation have broad implications including (1) application to the design of sound sources for deep sediment penetration, (2) applications relative to sediment recognition through interrogation with sound and (3) application to determination of acoustic behavior of sediments as related to resonance vibrations of man-made structures with sub-marine based foundations.

## 1.0 INTRODUCTION

This monograph describes work that was done by the writer to experimentally determine the acoustical transmission response of the first sedimentary layer below the ocean's bottom. The approach involved spectral analysis of magnetic tape recordings obtained during continuous seismic reflection profiling.

Continuous seismic reflection profiling has perhaps become the most useful method of determining the configuration of the ocean's bottom and the sedimentary layering below the bottom. Basically, the technique involves the periodic emission of sound pulses from a ship underway and the subsequent receiving back at the ship of the sound pulses as they are reflected from the ocean's bottom and the interfaces between sedimentary layers below the bottom. The arrival times of the reflected pulses provide a means of determining the relative spacing of the interfaces at a location below the ship. The reflected pulses are converted into electrical signals which are ultimately routed to a graphical recorder which provides a continuous record of the geological profile along the ship's track. Hersey<sup>2</sup> has written an excellent and much more detailed description of the methods and equipment used in continuous seismic reflection profiling.

During the past ten years, the methods and equipment used in continuous seismic reflection profiling have been greatly improved. So far as the writer has been able to discover, however, the arrival times of reflections are the only information that is utilized. The fact that appropriate filtering enhances the appearance of broad spectrum

reflected signals is clear indication that the spectral content of reflected signals could be used to determine the filtering characteristics of the sedimentary layers. As long ago as 1949, Hersey and Ewing<sup>3</sup> noted the changing spectral nature of broad spectrum reflections from successively deeper sedimentary interfaces. But since that time, no one has made use of that phenomenon to systematically determine the filtering characteristics of specific sedimentary layers in their in situ environment. It would seem that this shows promise as a means of determining the types and properties of sedimentary layers.

A number of highly correlated physical properties of sediments determine their acoustical behavior. These physical properties are porosity, median grain size, distribution of grain size, shape of grains, spatial relationship of grains, compressibility of grains, aggregate rigidity, and aggregate density. This has been demonstrated in both theoretical and empirical absorption studies by such workers as Ament,<sup>4</sup> Biot,<sup>5,6</sup> Shumway,<sup>7,8</sup> Urick,<sup>9</sup> and Wood and Weston.<sup>10</sup> These investigations considered frequencies that are much higher than those of interest in seismic reflection studies. For example, the experiments of Shumway were conducted in the 20 kcps to 37 kcps range, and those of Wood and Weston in the 4 kcps to 50 kcps range. The frequencies of interest in continuous seismic reflection studies are in the low hundreds of cycles per second. Furthermore, except for Wood and Weston, the above workers conducted their experiments on sediments in a laboratory rather than with in situ oceanic sediments. The experiments of Wood and Weston involved the transmission of sound between a source and receiver which were placed within a sedimentary layer. These experiments were not affected by

factors related to transmission and reflection at sedimentary interfaces, and the possible aggregate acoustical behavior of a sedimentary layer as a unit within its geological environment.

To mathematically model the acoustical filtering characteristics of sediments as a function of their above mentioned physical properties is obviously an overwhelming task. To predict the acoustical behavior of sedimentary layers in their natural oceanic environment where other, perhaps unknown, factors may appear is even more difficult. It would seem, then, that the development of an empirical approach such as was attempted in this investigation, would be of great value.

## 2.0 THEORETICS

### 2.1 Physical Model and Notation

Two separate electroacoustic transducers are involved--a sound source and a receiver. Their distances below the ocean's surface and their horizontal separation are quite small relative to the ocean's depth. The receiver is well astern of the ship (several hundred feet) to minimize engine noise and water flow noise from the ship. The geometry of this along with dimensional and other notation is shown in Figure 1. The experimental work described in this monograph dealt with the determination of the transmission response of the first layer of sediment below the ocean's bottom. The techniques can, however, be applied to lower layers.

### 2.2 Electroacoustic Transducers

#### 2.2.1 Sound Source

A number of different kinds of sound sources are used for seismic reflection profiling and have been discussed by Hersey.<sup>1</sup> The work treated herein is concerned with a source called the sparker. This device employs a high tension electrical spark discharged under water using from 4 to 100,000 joules of electrical energy stored in capacitors. Anywhere from 0.5 to 10 per cent of the electrical energy is converted into acoustical energy. The acoustical pressure wave emitted from a sparker is nearly omnidirectional and has the form shown in Figure 2. The time scale is approximate and varies with such parameters as discharged energy and

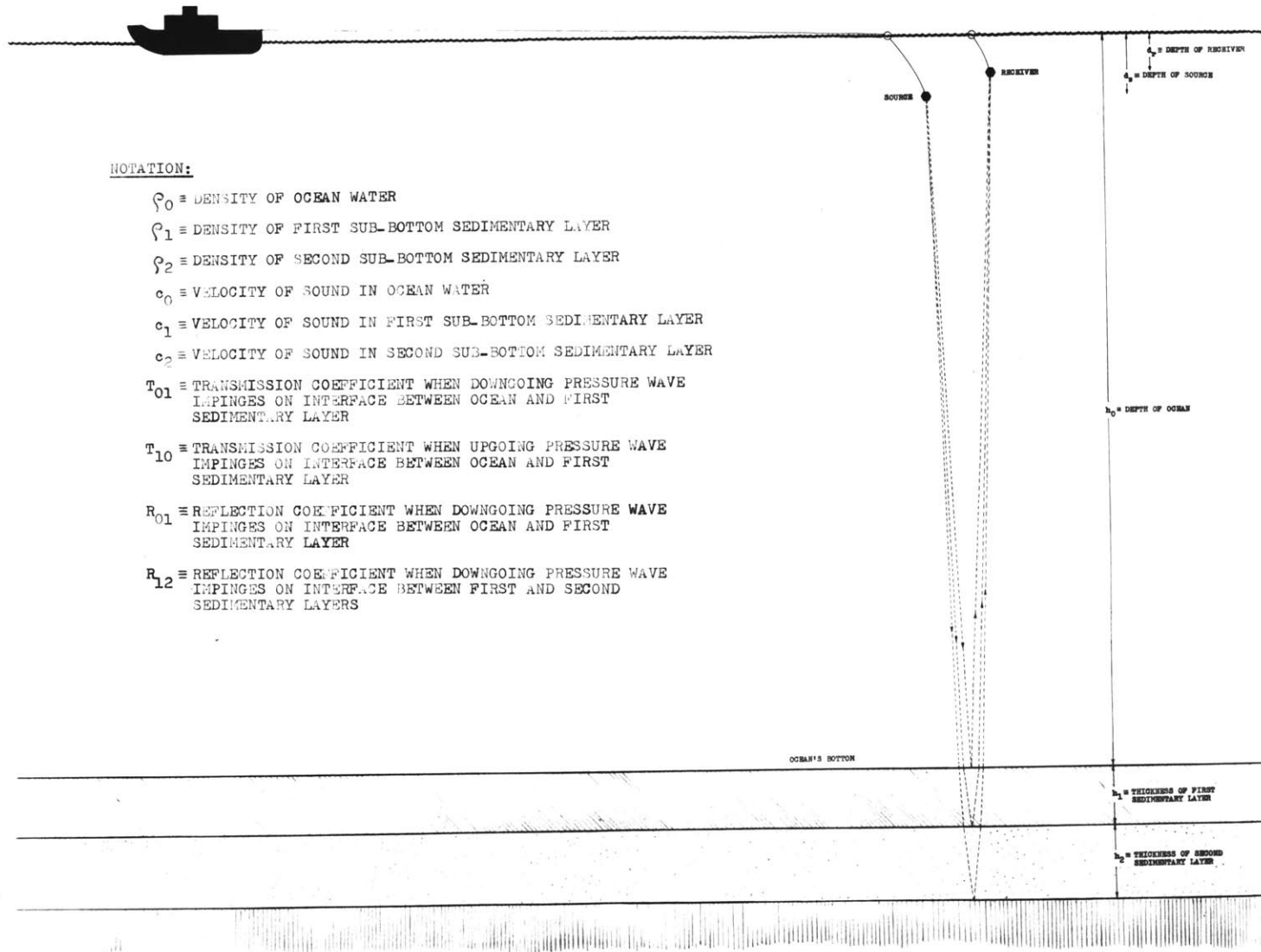


Figure 1. GEOMETRY AND NOTATION FOR PHYSICAL MODEL

depth below the ocean's surface.

The first pressure pulse at 0 milliseconds is the result of an initial bubble expansion following the electrical spark. About 20 milliseconds later, this bubble collapses at which time a second pressure pulse is emitted. The bubble expands and collapses perhaps twice more; and at the time of each collapse a pressure pulse is emitted. Moon<sup>11</sup> has used high speed stroboscopic photography to obtain pictures of a low energy underwater spark followed by the expanding and collapsing bubble.

Most of the energy of a sparker exists at frequencies equal to the reciprocal of the intervals between the pressure pulses shown in Figure 2. That is, most of the energy is present within a spectral range in the low hundreds of cycles per second, although some energy is present at frequencies ranging in the low thousands of cycles per second. These frequencies seem to represent an optimum tradeoff between resolution and sediment penetration up to several thousands of feet. The fact that the frequency spectrum is so wide is quite useful since experience has shown that no single frequency is consistently optimum to obtain desired reflections. Appropriate filtering accomplishes desired results for different needs.

#### 2.2.2 Receiver

A wide range of receivers are used. They are either piezoelectric or magnetostriction hydrophones. In their region of flat frequency response these devices provide a voltage proportional to absolute pressure. Hydrophones are used singularly or in arrays.

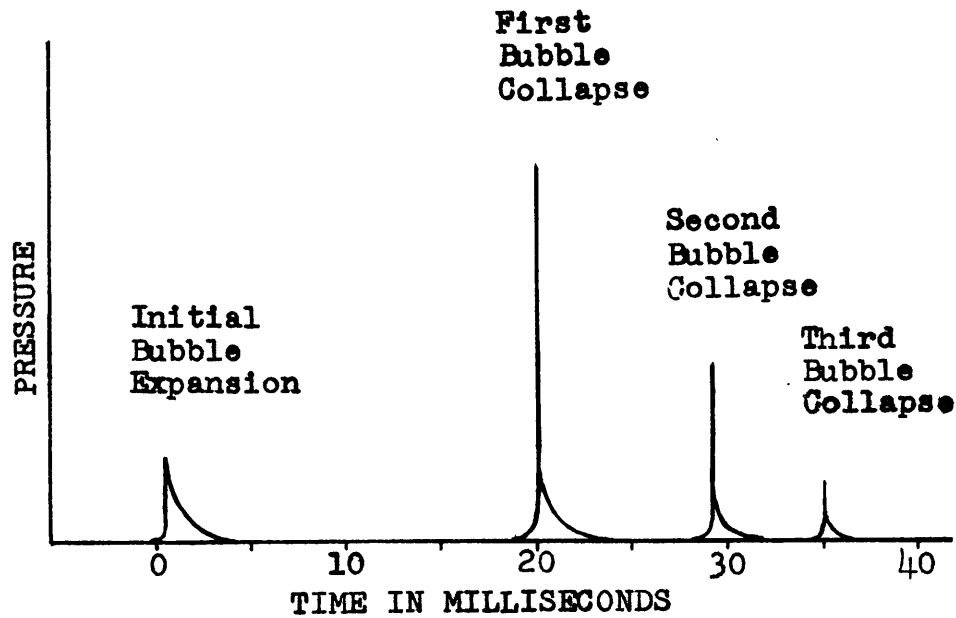


Figure 2. PRESSURE WAVE FROM A SPARKER

### 2.3 Mathematical Models

#### 2.3.1 Reflection and Transmission at Interfaces

The empirical work described later involved an ocean depth of nearly 3000 feet and flat sedimentary layering. This circumstance makes it possible to treat the problem as one involving normally incident plane waves. The frequencies of interest ranged between 75 and 600 cps, which give wavelengths in the water ranging from 65 down to 8 feet. Wavelengths this large and relatively smooth interfaces make it reasonable to consider reflection and transmission at the interfaces to be specular and frequency independent.

An acoustic wave impinging on the interface between medium  $i$  and medium  $j$  from the direction of medium  $i$ , will be partially

reflected and partially transmitted. The amplitude of the reflected wave is given by the product of the amplitude of the impinging wave and the reflection coefficient  $R_{ij}$ . Similarly, the amplitude of the transmitted wave is given by the produce of the amplitude of the impinging wave and the transmission coefficient  $T_{ij}$ . Under the conditions described in the above paragraph, the reflection and transmission coefficients are determined by the following well known equations (see, for example, references 12 and 13).

$$(1) \quad R_{ij} = \frac{\rho_j c_j - \rho_i c_i}{\rho_j c_j + \rho_i c_i}$$

$$(2) \quad T_{ij} = \frac{2\rho_i c_j}{\rho_j c_j + \rho_i c_i}$$

where:

$\rho_i, \rho_j \equiv$  Densities of mediums i and j

$c_i, c_j \equiv$  Velocities of sound in mediums i and j

The product  $\rho c$  is known as the acoustical impedance of a medium. If a sound wave strikes an interface between two mediums of different acoustical impedance, the reflection coefficient in equation (1) will obviously be positive or negative depending upon which direction the wave is traveling. If the reflection coefficient is positive the impinging and reflected waves will be of the same phase. If the reflection coefficient is negative, there will be a 180 degree phase shift.

In the case of sedimentary layering, it is most common to find increasing acoustical impedance with increasing depth. Thus, down-going and reflected waves generally have the same phase. When sound waves in the ocean strike the water/air interface at the ocean's surface, there is a 180 degree phase shift because of the lower acoustical impedance of the air. In fact, the acoustical impedance of air is so much lower than that of water that the reflection coefficient very nearly equals -1. For the long acoustic wavelengths involved in this study, it appears reasonable to treat the ocean's surface as smooth, thus resulting in specular reflection.

### 2.3.2 Spreading Loss

It is well known that the energy per unit area decreases inversely with the square of the distance from the source. The instantaneous energy in an acoustical wave is proportional to the square of the amplitude of the pressure. Thus, the amplitude of a pressure wave as measured by a hydrophone decreases inversely with distance (not the square of the distance) from the source. Horton<sup>14</sup> has treated this matter in more detail.

In calculating spreading loss, refraction at sedimentary interfaces must be considered. Figure 3 shows the path of a sound ray reflecting off of the first sedimentary interface below the ocean's bottom. Because of refraction, the wave appears to have been reflected from an imaginary interface below the real interface. Thus, for purposes of calculating the spreading loss, the layer should be

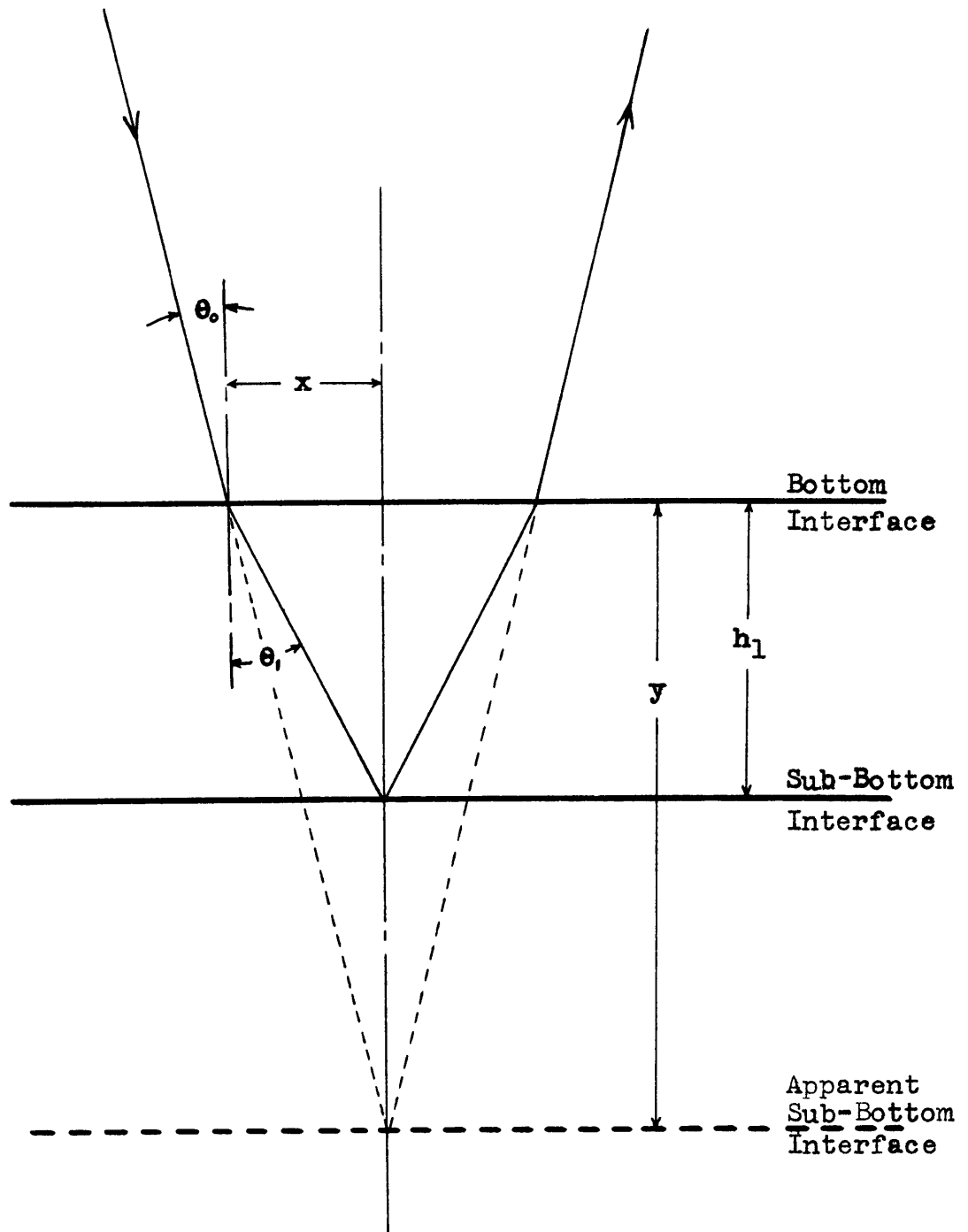


Figure 3 - SPREADING LOSS GEOMETRY

considered to have a thickness  $y$  instead of  $h_1$  as shown in Figure 3.

The solution for  $y$  is as follows.

The distance  $x$  is given by

$$(3) \quad x = h_1 \tan \theta_1 = y \tan \theta_0$$

Snell's Law says that

$$(4) \quad \frac{c_0}{\sin \theta_0} = \frac{c_1}{\sin \theta_1}$$

Substitution of equation (4) into equation (3) together with appropriate use of trigonometric identities gives

$$(5) \quad y = \left[ h_1 \frac{c_1}{c_0} \right] \left[ \frac{1 - \sin^2 \theta_0}{1 - \frac{c_1}{c_0} \sin^2 \theta_0} \right]^{\frac{1}{2}}$$

For normal incidence  $\theta_0 = 0$ , which reduces equation (5) to

$$(6) \quad y = h_1 \frac{c_1}{c_0}$$

### 2.3.3 Attenuation

Officer<sup>13</sup> presents an empirically obtained equation for attenuation in sea water. It is

$$(7) \quad \alpha = 0.20 f + 0.00015 f^2 \text{ db/kyd}$$

where  $f$  is in kilocycles per second. It has been stated that the frequencies of interest in this study ranged between 75 and 600 cps; and

that the ocean depth was nearly 3000 feet. Under these conditions, equation (7) shows that the total attenuation for a sound wave traveling from the surface to the bottom and back experiences attenuations ranging from 0.03 to 0.24 db. This is negligible compared with attenuations in the sediments and can, therefore, be eliminated from consideration.

Sound passing through a sedimentary layer is attenuated. This results from absorption, scattering, and perhaps other effects. Absorption is the conversion of sound energy into heat through frictional losses. Scattering is the modification of sound direction within the sediment due to innumerable reflections at the particle level. In this monograph, attenuation is meant to include all forms of signal diminishment except spreading loss.

#### 2.3.4 Energy Spectrums of Seismic Reflections

The empirical work described later in this monograph was primarily aimed at determining the acoustical transmission response of the first sedimentary layer below the ocean's bottom. In particular, it was desired to work in the frequency domain so as to plot the acoustical attenuation of the sedimentary layer as a function of frequency. The mathematical models describing the energy spectrums for seismic reflections are developed below.

The source generates some pressure wave  $sp(t)$  whose Fourier transform is  $SP(\omega)$ . The reflection of this wave off of each sedimentary interface arrives at the receiver via four different paths as illustrated in Figure 4.

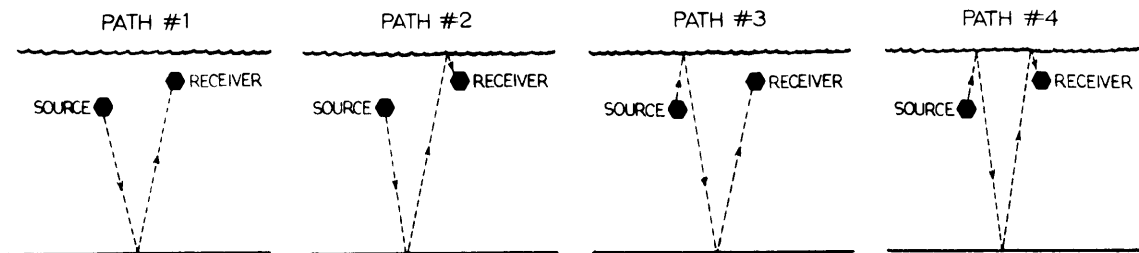


Figure 4. MULTIPLE SOUND ARRIVAL PATHS

The arrivals of  $sp(t)$  at the receiver via paths #2, #3 and #4 lag the arrival via path #1 by  $2d_s/c_o$ ,  $2d_r/c_o$  and  $(2d_r+2d_s)/c_o$ , respectively. The quantities  $d_s$ ,  $d_r$  and  $c_o$  are defined in Figure 1.

Delaying a time function by an amount  $t_o$  has the effect of multiplying its frequency spectrum by  $e^{-j\omega t_o}$ . Thus, the Fourier transform  $SP(\omega)$  must be multiplied by the appropriate factors which account for the above time lags in order to determine the Fourier transform of the total sound wave arriving at the receiver.

The Fourier transform  $RP_{01}(\omega)$  of the pressure wave  $rp(t)$  arriving at the receiver from the sedimentary interface at the ocean's bottom is now easily derived and is shown in equation (8). This equation takes account of (1) the four different path lengths shown in Figure 4 for purposes of calculating spreading losses and the effects of time delays on frequency spectrums (2) the fact that there is a 180 degree phase shift for a reflection from the ocean's surface and (3) the reflection coefficient  $R_{01}$  at the ocean's bottom.

$$(8) \quad RP_{01}(\omega) = R_{01} \left[ \frac{1}{2h_o - d_s - d_r} - \frac{e^{-j\omega \frac{2d_s}{c_o}}}{2h_o + d_s - d_r} - \frac{e^{-j\omega \frac{2d_r}{c_o}}}{2h_o - d_s + d_r} + \frac{e^{-j\omega \frac{2d_r + 2d_s}{c_o}}}{2h_o + d_s + d_r} \right] SP(\omega)$$

In equation (8) and henceforth, zero time is arbitrarily established at the point of first arrival of sound from the ocean's bottom.

The Fourier transform  $RP_{12}(\omega)$  of the pressure wave  $rp_{12}(t)$  arriving at the receiver from the first sub-bottom sedimentary interface is easily derived in a manner similar to that for equation (8). This time, however, additional account must be taken of (1) the transmission response  $H_1(\omega)$  of the first sedimentary layer through which the sound passes (2) the transmission and reflection coefficients  $T_{01}$ ,  $T_{10}$  and  $R_{12}$  as defined in Figure 1 and (3) the adjustment to spreading loss in the sedimentary layer resulting from refraction as indicated in equation (6). The solution for  $RP_{12}(\omega)$  is

$$(9) \quad RP_{12}(\omega) = T_{01} R_{12} T_{10} \left[ \frac{e^{-j\omega \frac{2h_1}{c_1}}}{2h_o + 2h_1 \frac{c_1}{c_o} - d_s - d_r} - \frac{e^{-j\omega \left( \frac{2h_1}{c_1} + \frac{2d_s}{c_o} \right)}}{2h_o + 2h_1 + d_s - d_1} - \frac{e^{-j\omega \left( \frac{2h_1}{c_1} + \frac{2d_r}{c_o} \right)}}{2h_o + 2h_1 \frac{c_1}{c_o} - d_s + d_r} + \frac{e^{-j\omega \left( \frac{2h_1}{c_1} + \frac{2d_s + 2d_r}{c_o} \right)}}{2h_o + 2h_1 \frac{c_1}{c_o} + d_s + d_r} \right] SP(\omega) H_1(\omega)$$

For the case under consideration  $h_o$  is much larger than  $d_s$  and  $d_r$ . Thus, equations (8) and (9) reduce to

$$(10) \quad RP_{01}(\omega) = \frac{R}{2h_o} \left[ \begin{array}{ccc} & -j\omega \frac{2d_s}{c_o} & -j\omega \frac{2d_r}{c_o} \\ 1 - e & - e & + e \end{array} \frac{2d_s + 2d_r}{c_o} \right] SP(\omega)$$

$$(11) \quad RP_{12}(\omega) = \frac{T_{01}R_{12}T_{10}}{2h_o + 2h_1 \frac{c_1}{c_o}} \left[ \begin{array}{ccc} & -j\omega \frac{2h_1}{c_1} & -j\omega \left( \frac{2h_1}{c_1} + \frac{2d_s}{c_o} \right) \\ e & - e & - e \end{array} \frac{2d_s + 2d_r}{c_o} \right] SP(\omega) H_1(\omega)$$

The energy spectrums of the reflections from the bottom and sub-bottom interfaces are given by the square of the absolute value of equations (10) and (11). Setting  $\omega = 2\pi f$ , they are:

$$(12) \quad |RP_{01}(2\pi f)|^2 = \left[ \frac{R_{01}}{h_o} \right]^2 \left[ 1 - \cos\left(\frac{4\pi d_s}{c_o} f\right) \right] \left[ 1 - \cos\left(\frac{4\pi d_r}{c_o} f\right) \right] \left| SP(2\pi f) \right|^2$$

(13)

$$|RP_{12}(2\pi f)|^2 = \left[ \frac{T_{01}R_{12}T_{10}}{h_o + h_1 \frac{c_1}{c_o}} \right]^2 \left[ 1 - \cos\left(\frac{4\pi d_s}{c_o} f\right) \right] \left[ 1 - \cos\left(\frac{4\pi d_r}{c_o} f\right) \right]$$

$$\cdot |SP(2\pi f)|^2 |H_1(2\pi f)|^2$$

The factors  $\left[ 1 - \cos\left(\frac{4\pi d_s}{c_o} f\right) \right]$  and  $\left[ 1 - \cos\left(\frac{4\pi d_r}{c_o} f\right) \right]$

in equations (12) and (13) appear because of the reflections from the ocean's surface. It will be noted that they predict maximum interference at frequencies of  $f = nc_o/2d_s$  and  $f = nc_o/2d_r$ , where  $n = 0, 1, 2, 3 \dots$

### 2.3.5 Transmission Response of First Sedimentary Layer

Solutions of equations (12) and (13) for the square of the absolute value of the transmission response of the first sedimentary layer below the ocean's bottom gives

$$(14) \quad |H_1(2\pi f)|^2 = \left| \frac{h_o + h_1 \frac{c_1}{c_o}}{h_o} \frac{R_{01}}{T_{01}R_{12}T_{10}} \right|^2 \frac{|RP_{12}(2\pi f)|^2}{|RP_{01}(2\pi f)|^2}$$

The attenuation of a filter in decibels is defined (see, for example, Mason and Zimmerman<sup>15</sup>) as follows:

$$(15) \quad \alpha = -10 \log_{10} |H(\omega)|^2$$

where:  $H(\omega) \equiv$  Frequency domain transmission response of the filter.

Applying this to equation (14), the attenuation of the first sedimentary layer below the ocean's bottom becomes

$$(16) \alpha = -20 \log_{10} \left| \frac{h_o + h_1 \frac{c_1}{c_o}}{h_o} \frac{R_{01}}{T_{01}R_{12}T_{10}} \right| - 10 \log_{10} \frac{|RP_{12}(2\pi f)|^2}{|RP_{01}(2\pi f)|^2}$$

The first term on the right hand side of equation (16) is frequency independent according to assumptions made earlier. It, therefore, becomes a constant reference level on a frequency response curve (i.e., a plot of  $\alpha$  vs.  $f$ ). A numerical value for the first term cannot be obtained from the seismic reflections only since none of the parameters in this term can be determined without additional independently obtained information.

The second term on the right hand side of equation (16) can be determined from the seismic reflections. This term is frequency dependent. The fortunate result, then, is that even if precise velocities, ocean depth, sediment thickness, and transmission and reflection coefficients remain unknown, it is still possible to determine how sediment attenuation varies with frequency relative to some constant level. It would appear that this is the pertinent information for purposes outlined in the introduction to this monograph.

### 3.0 EMPIRICS

#### 3.1 Original Data

Both graphic and magnetic tape recordings are nearly always simultaneously made during the continuous seismic reflection profiling done from the research vessels of the Woods Hole Oceanographic Institution. A great many such recordings were carefully examined to locate suitable seismic returns for this study. The requirements for a "suitable" return include (1) that the return consist of normal incidence reflections from a well defined bottom interface and one sub-bottom interface; i.e., the interfaces must be horizontal and represent abrupt changes between types of medium (2) that the return have a relatively high signal-to-noise ratio, say five to one and (3) that the ocean depth be shallow enough and the sedimentary layer be unconsolidated and thin enough to represent a research situation that would have certain practical applications. Items (1) and (2) above lead to a tractable mathematical treatment as covered in part 2.0 of this monograph. Item (3) contemplates effort relative to such things as commercial deposits of minerals, sand and gravel, and so forth; and civil engineering projects involving foundations on the ocean's bottom.

Two seismic returns were finally selected for detailed analysis. They were recorded in an area of the Red Sea during cruise #43 of the research vessel Chain. The recordings were made along profile #3 on 22 March 1964 between the hours of 2320 and 2335. The ship was

moving in a southerly direction at a geographical location of approximately  $26.09^{\circ}$  North and  $35.43^{\circ}$  East. The geological profile along the track indicated above as recorded by a PGR (Precision Graphic Recorder) is shown in Figure 5. The data interval indicated above is marked on this figure. Unconsolidated sediments comprise the first layer below the ocean's bottom.

The sound source was a sparker operating at 8.4 kilovolts and an intended depth of 20 feet. The receiver was the so-called Chesapeake hydrophone array towed 300 feet astern of the ship at an intended depth of 12 feet. The seismic reflections were simultaneously recorded by the PGR and by a quarter-track four-channel Crown model 800 tape recorder at 3-3/4 inches per second.

### 3.2 Signal Processing

For this study, the original tape recorded data was played on a Crown model 800 tape recorder and re-recorded using a quarter-track two-channel Magnecord model 1024 tape recorder. This transfer was accomplished at the Woods Hole Oceanographic Institution, and greatly facilitated subsequent signal processing which involved work in Prof. H. E. Edgerton's Strobe Lab at the Massachusetts Institute of Technology. Problems overcome by the transfer included (1) the undesirability of removing the original magnetic tapes from the Woods Hole premises (2) the difficulty in obtaining a tape recorder with the necessary features to play the original recordings in the Strobe Lab and (3) the undesirability of altering the original

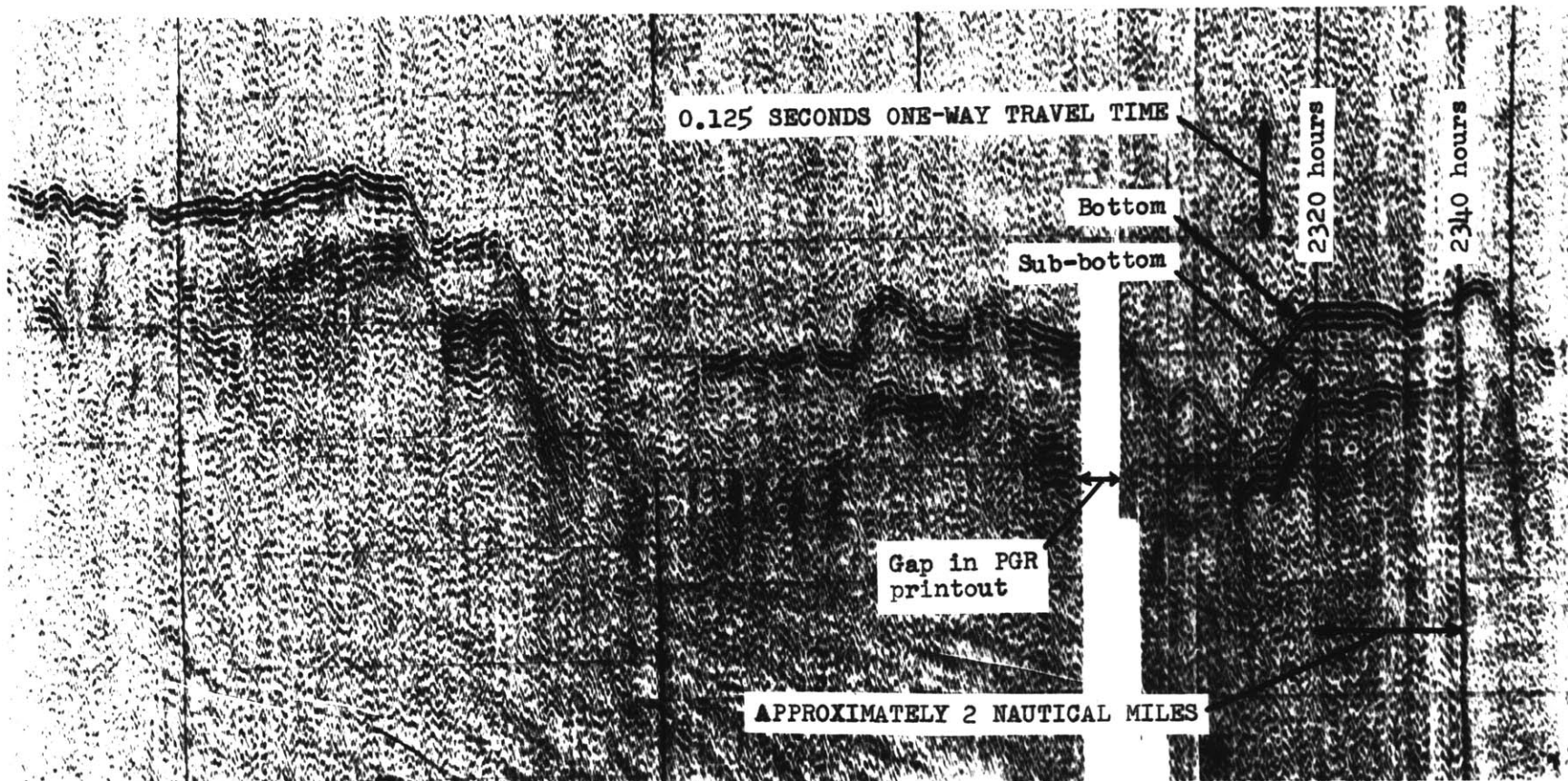


Figure 5 - SEISMIC REFLECTION PROFILE IN AN AREA OF THE RED SEA  
(BAND-PASS FILTERING BETWEEN 31 AND 75 cps)

recording for purposes of identifying certain reflections.

The re-recorded seismic reflections were played on the Magnecord recorder into a Tektronix oscilloscope and photographed. Fast oscilloscope sweep rates were often used such that only a small portion of a total seismic return appeared on the screen. In these cases, the same return was played many times; and each time the sweep was appropriately delayed such that a series of oscillograms were made which, when placed end to end, constituted a complete picture of the seismic return.

The oscillograms of the two selected seismic returns were digitized at a sampling frequency of 5000 cps on the Benson-Lehner oscillogram reader at the Woods Hole Oceanographic Institution. The digitized signals were then mathematically treated by an RCA Model 301 Computer at the RCA Aerospace Systems Division in Burlington, Massachusetts. The program used on the computer was designed to provide solutions for the energy spectrums of the bottom and sub-bottom reflections for each of the two seismic returns that were analyzed. Additionally, the computer solved for minus ten times the common logarithm of the ratio of the energy spectrums. This represents the frequency dependent part of the attenuation in the first sedimentary layer which appears as the second term in equation (16). In the notation used earlier, then, the computer solved for  $|RP_{01}(2\pi f)|^2$ ,  $|RP_{12}(2\pi f)|^2$ , and  $-10 \log_{10} [ |RP_{12}(2\pi f)|^2 / |RP_{01}(2\pi f)|^2 ]$ . The computer calculated points on the energy spectrum curves using the equation developed below.

The Fourier transform of any time function  $g(t)$  is given by

$$(17) \quad G(2\pi f) = \int_{-\infty}^{\infty} g(t) e^{-j2\pi ft} dt$$

$$= \int_{-\infty}^{\infty} g(t) \cos(2\pi ft) dt - j \int_{-\infty}^{\infty} g(t) \sin(2\pi ft) dt$$

The energy spectrum of the time function  $g(t)$  is given by

$$(18) \quad |G(2\pi f)|^2 = \left[ \int_{-\infty}^{\infty} g(t) \cos(2\pi ft) dt \right]^2 + \left[ \int_{-\infty}^{\infty} g(t) \sin(2\pi ft) dt \right]^2$$

If  $g(t)$  is digitized at some sampling frequency  $f_s$ , then the solution for the energy spectrum of  $g(t)$  is obtained by evaluating the following digital version of equation (18).

$$(19) \quad |G(2\pi f_n)|^2 = \left[ \sum_{n=0}^N g(n/f_s) \cdot \cos(2\pi f_n n/f_s) \cdot 1/f_s \right]^2$$

$$+ \left[ \sum_{n=0}^N g(n/f_s) \cdot \sin(2\pi f_n n/f_s) \cdot 1/f_s \right]^2$$

In equation (19),  $g(n/f_s)$  is the value of  $g(t)$  at the points where digital values were obtained; the cosine and sine terms are evaluated at the points where digital values of  $g(t)$  were obtained; and  $1/f_s$  is the time interval between sample points. Evaluation of equation (19) must be accomplished for each  $f_n$  where a point on the energy spectrum is desired. The summation over  $n=0$  to  $N$  accomplishes a numerical integration over a time interval  $N/f_s$ .

Equation (19) was used to provide numerical solutions for  $|RP_{01}(2\pi f)|^2$  and  $|RP_{12}(2\pi f)|^2$ . For the evaluations, the sampling frequency  $f_s$  was 5000 samples per second. Numerical solutions for points

$f=f_n$  on the energy spectrum curves were obtained every five cycles for frequencies ranging from 50 to 2500 cycles per second. The summation  $n=0$  to  $N$  accomplished a numerical integration over a time interval  $N/f_s$  equal to the duration of the appropriate reflection.

The fact that the main intention in this study was to calculate the transmission response of the first sedimentary layer has simplified the mathematical treatment of the signals as described above. That is, compensating factors did not have to be, and were not, introduced to account for other than flat frequency responses of the various electronic equipments through which the signals passed. The reason for this is that in a single seismic return both the bottom and sub-bottom reflections experience the same signal processing. Thus, any spectral modifications introduced by the hydrophones, tape recorders, amplifiers and so forth, cancel out in the ratio of the energy spectrums of the recorded bottom and sub-bottom reflections.

### 3.3 Results

#### 3.3.1 Oscillograms of the Seismic Returns

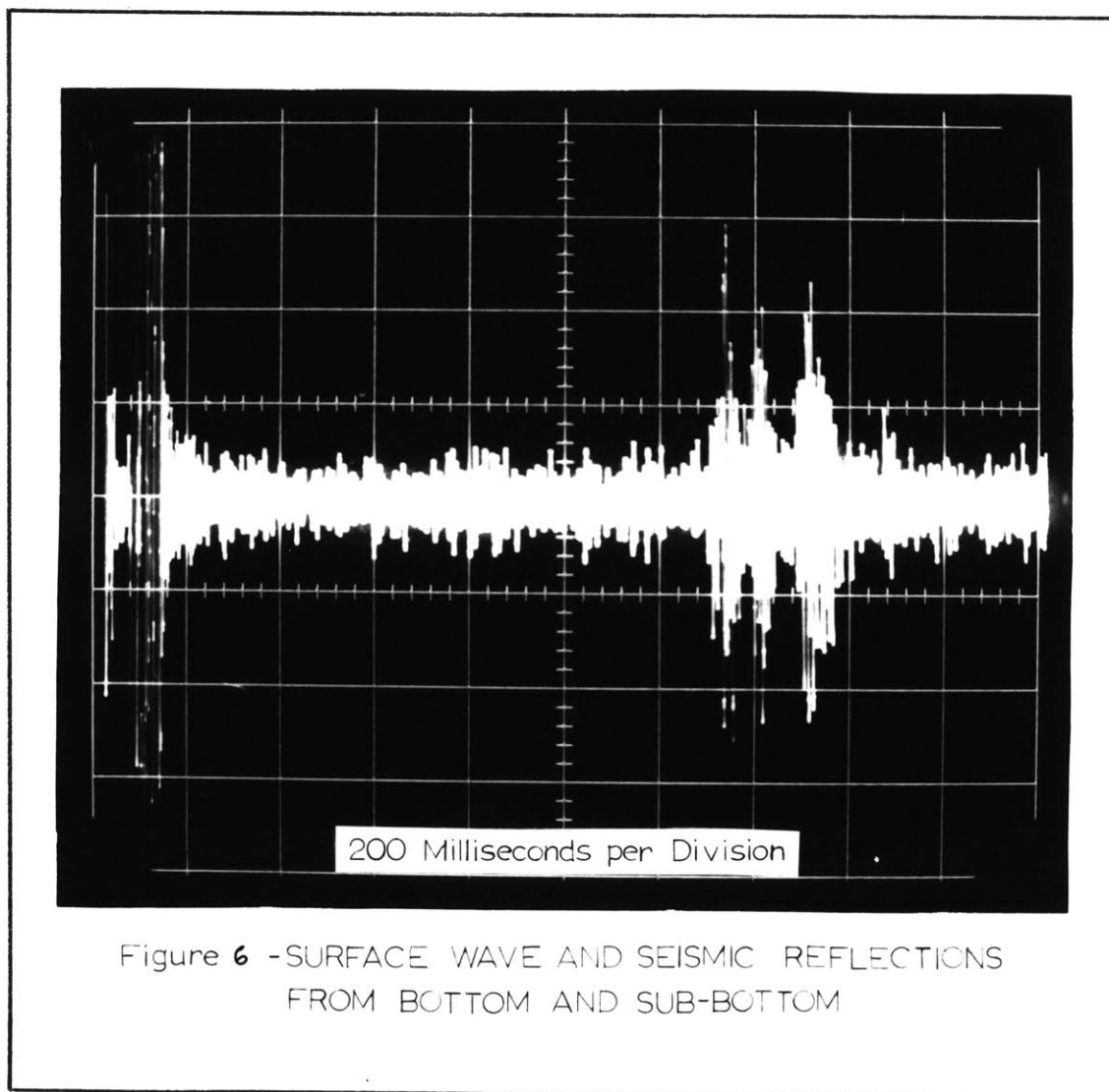
As stated earlier, two seismic returns (hereinafter designated as returns #1 and #2) were selected for detailed analysis. Oscillograms of return #1 appear in Figures 6 through 10. These five oscillograms were all made using different oscilloscope sweep rates. The oscillograms of return #2 are not included in this monogram. One oscillogram of a return other than the two selected for analysis appears in Figure 11. In all of the oscillograms it will be noted that the sound pulses

resulting from the initial bubble expansion and from the bubble collapse do not have the appearance of those in Figure 2. This is primarily the result of the frequency response of the tape recorders which have a differentiating effect at low frequencies.

The oscilloscope sweep in Figure 6 was triggered at the time of the sparker discharge. The direct arrival of the sound pulse appears at the hydrophone array 60 milliseconds later. The bottom reflection arrives at the hydrophone array 1280 milliseconds after the sparker discharge. A water depth of 3072 feet is thus indicated by using a sound speed in water equal to 4800 feet per second and by remembering that the 1280 milliseconds is a two-way travel time. Two sub-bottom reflections clearly appear in Figures 6, 7, and 9. The second sub-bottom reflection is off the scale in Figures 8 and 10.

The first sub-bottom reflection appears quite clearly and is labeled in the PGR printout shown in Figure 5. Examination of Figure 9 shows a one-way travel time in the first sub-bottom sedimentary layer equal to 0.069 seconds. This gives a thickness of 400 feet using the reasonable assumed sound velocity of 5800 feet per second.

The second sub-bottom reflection was present in nearly all of the returns that were examined on the oscilloscope; however, it is barely discernable (and is not labeled) on the PGR record shown in Figure 5. The reason for this no doubt is the 31 to 75 cps band-pass filtering that was used for the PGR printout. This band-pass filtering would probably remove most of the second sub-bottom reflection which is nearly a 200 cps sine wave as can be seen in Figure 9. The unusual appearance



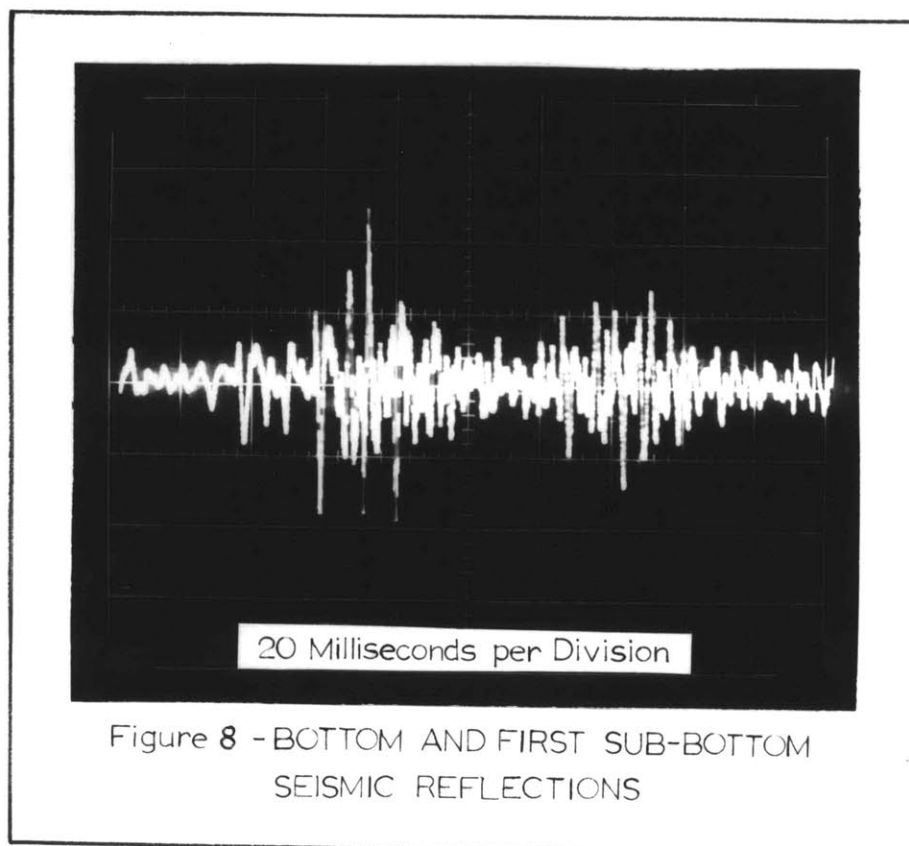
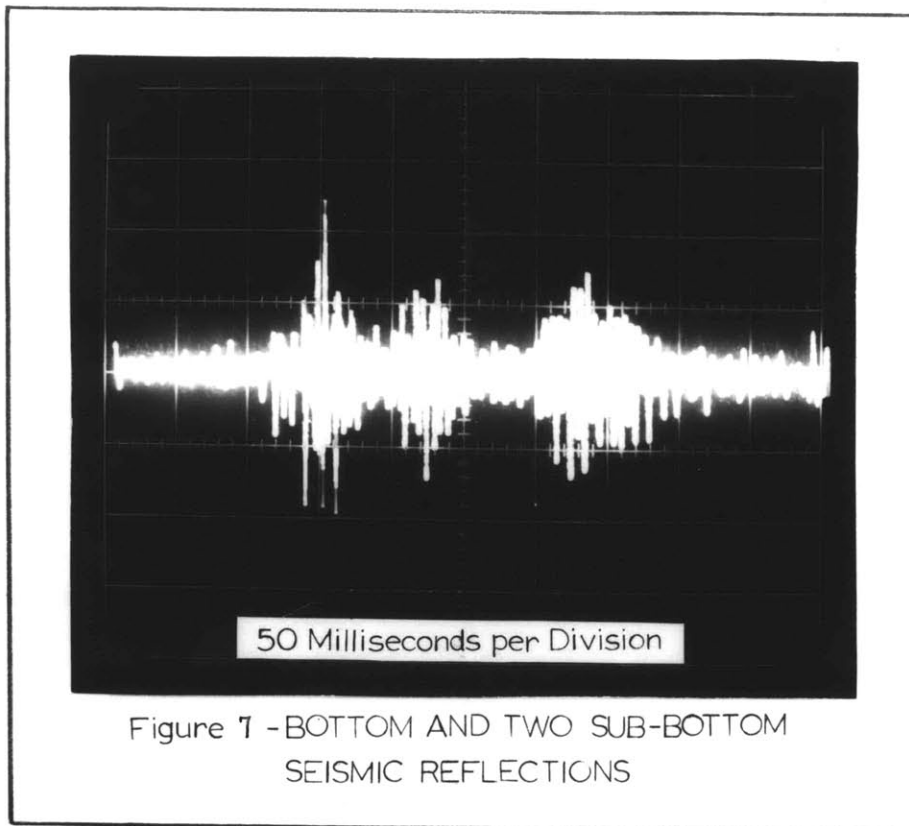


Figure 9

SEISMIC RETURN WITH HIGH-PASS FILTERING

(DOWN 3 db AT 75 cps)

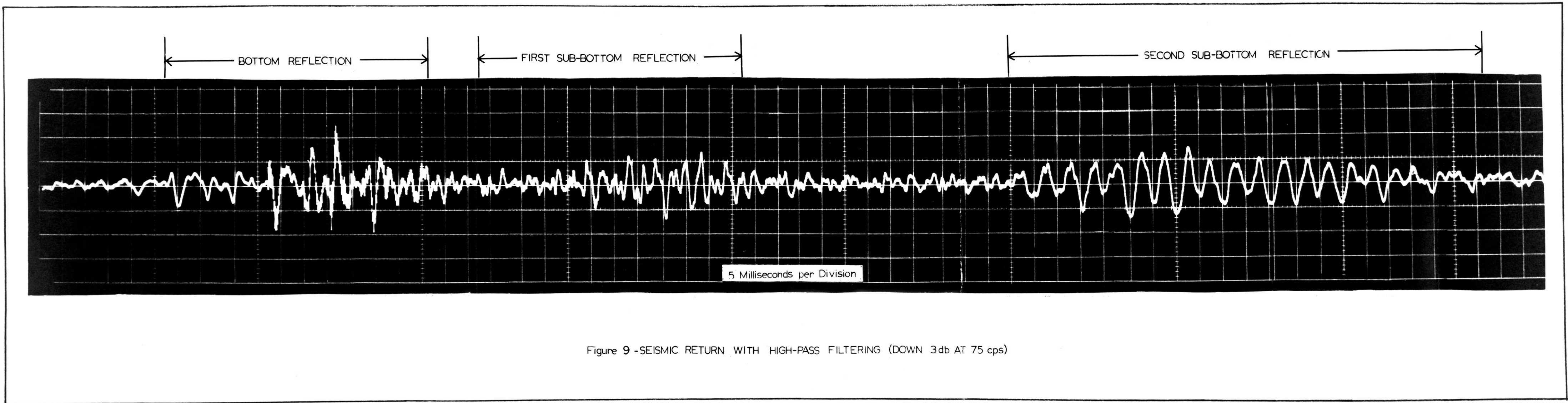
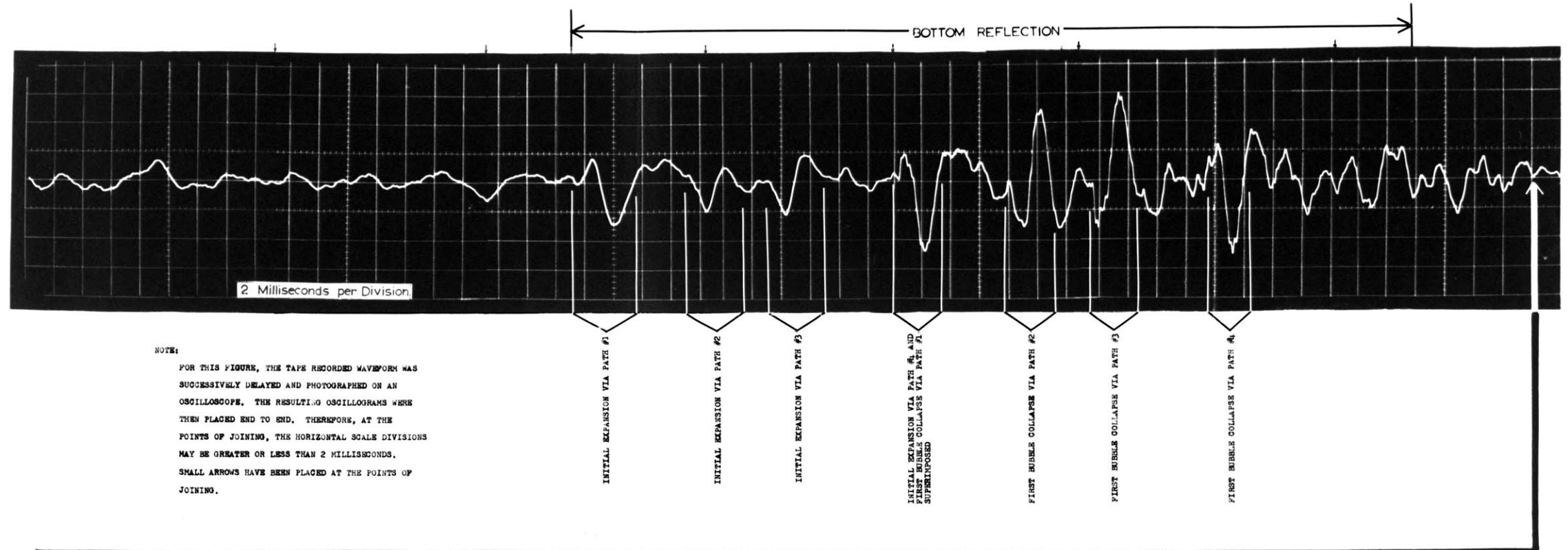


Figure 10

SEISMIC RETURN WITH BAND-PASS FILTERING

(DOWN 3 db AT 75 AND 3600 cps)



NOTE:  
 FOR THIS FIGURE, THE TAPE RECORDED WAVEFORM WAS SUCCESSIVELY DELAYED AND PHOTOGRAPHED ON AN OSCILLOSCOPE. THE RESULTING OSCILLOGRAMS WERE THEN PLACED END TO END. THEREFORE, AT THE POINTS OF JOINING, THE HORIZONTAL SCALE DIVISIONS MAY BE GREATER OR LESS THAN 2 MILLISECONDS. SMALL ARROWS HAVE BEEN PLACED AT THE POINTS OF JOINING.

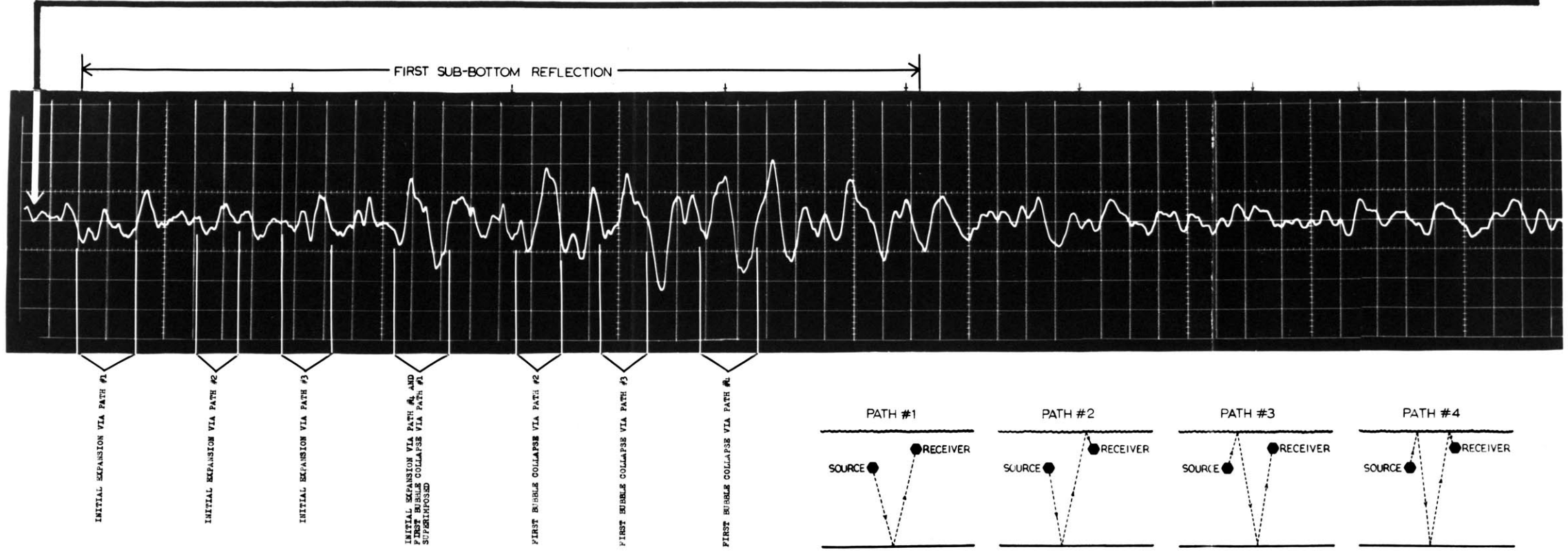
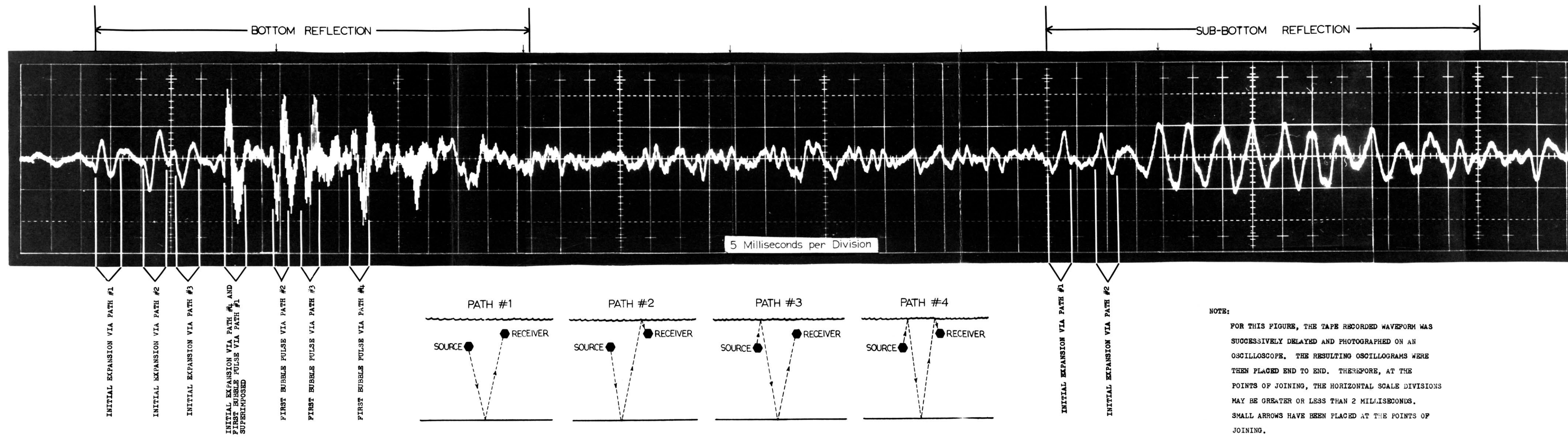


Figure 10 - SEISMIC RETURN WITH BAND-PASS FILTERING (DOWN 3 db AT 75 AND 3600 cps)

Figure 11

SEISMIC RETURN WITH HIGH-PASS FILTERING

(DOWN 3 db AT 67.5 cps)



NOTE:  
 FOR THIS FIGURE, THE TAPE RECORDED WAVEFORM WAS SUCCESSIVELY DELAYED AND PHOTOGRAPHED ON AN OSCILLOSCOPE. THE RESULTING OSCILLOGRAMS WERE THEN PLACED END TO END. THEREFORE, AT THE POINTS OF JOINING, THE HORIZONTAL SCALE DIVISIONS MAY BE GREATER OR LESS THAN 2 MILLISECONDS. SMALL ARROWS HAVE BEEN PLACED AT THE POINTS OF JOINING.

Figure II - SEISMIC RETURN WITH HIGH-PASS FILTERING (DOWN 3 db AT 67.5 cps)

first sub-bottom reflection is not present, or is at least very weak. Second, and even more interesting, is the fact that the initial bubble expansions appearing in the bottom and second sub-bottom reflections are  $180^{\circ}$  out of phase. This indicates a decreasing acoustical impedance with depth which is somewhat unusual.

### 3.3.2 Energy Spectrums of the Seismic Reflections

The initial bubble expansion in Figure 10 clearly appears in the bottom reflection; whereas, in the first sub-bottom reflection it is very difficult, if not impossible, to find because of its small amplitude. It was decided, therefore, to treat the reflections as beginning at the first bubble collapse arriving via path #1 and ending at the second bubble collapse arriving via path #4 as shown in Figure 10. The second bubble collapse is not actually labeled on the oscillogram; but, it occurs at the end of the reflections as shown in Figure 10. In other words, the energy spectrums of the seismic reflections were calculated for the waveforms between the first bubble collapse arriving via path #1 and the end of the reflection as shown in Figure 10. Additionally, it must be remembered that the calculated energy spectrums were of signals that were band-pass filtered between 75 and 3600 cps. The spectrums that were calculated from the oscillogram in Figure 10 appear in Figure 12. The energy spectrums for the other return that was analyzed appear in Figure 13.

The spectrums in Figures 12 and 13 indicate three main concentrations of energy. The first large concentration falls at 185 cps in

Figure 12

ENERGY SPECTRUMS OF BOTTOM AND SUB-BOTTOM SEISMIC REFLECTIONS #1

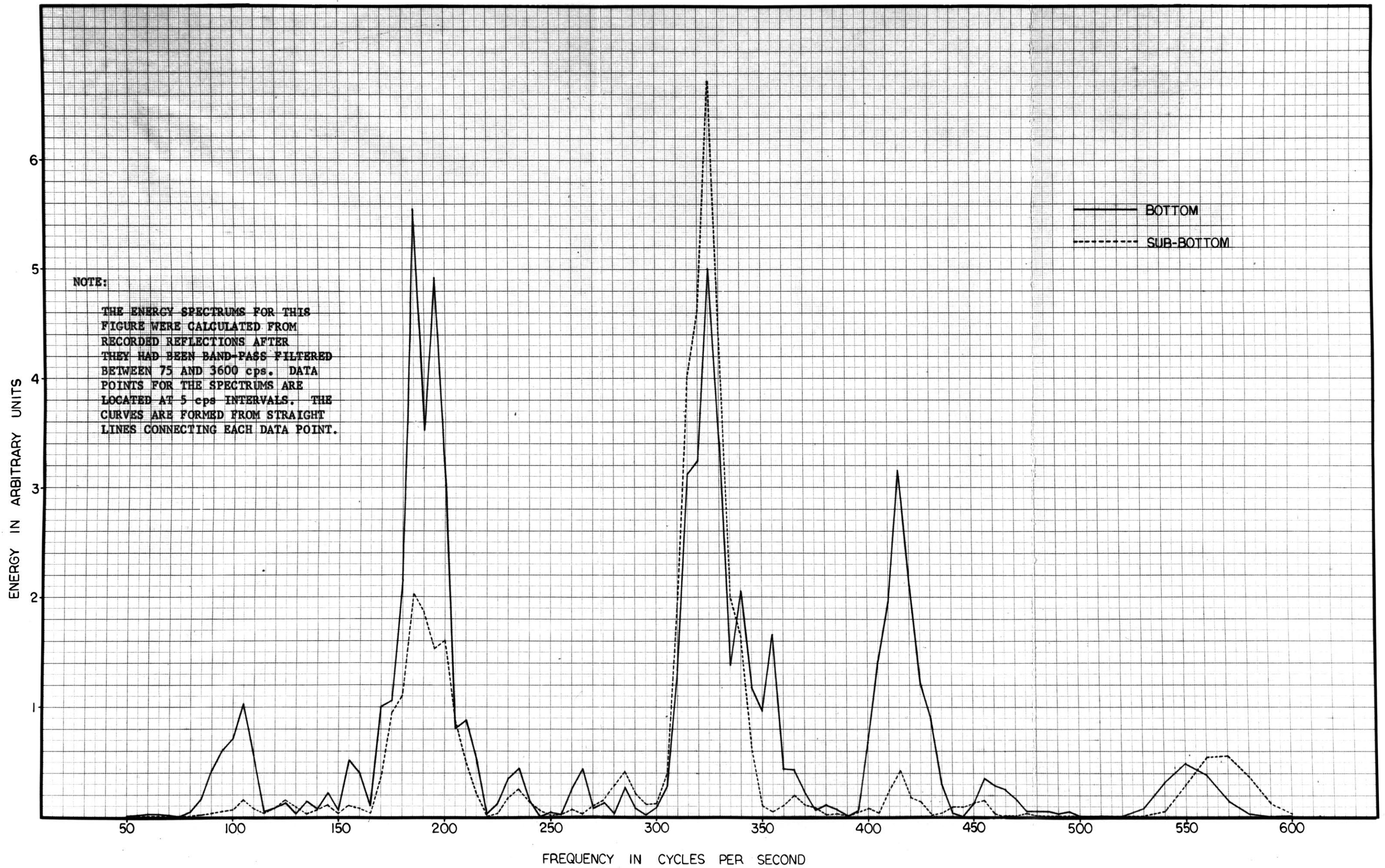


Figure 12 - ENERGY SPECTRUMS OF BOTTOM AND SUB-BOTTOM SEISMIC REFLECTIONS #1

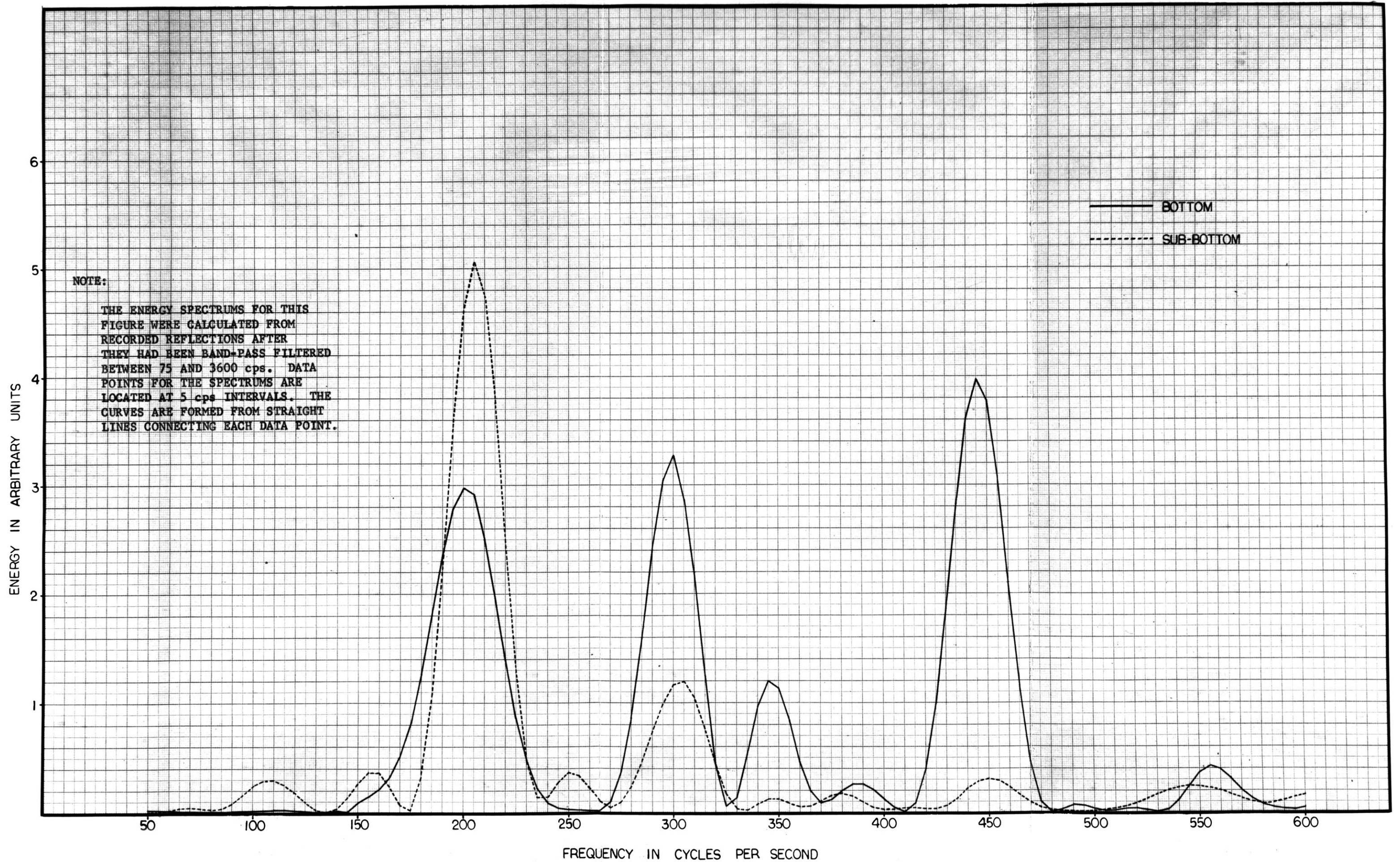


Figure 13 - ENERGY SPECTRUMS OF BOTTOM AND SUB-BOTTOM SEISMIC REFLECTIONS #2

Figure 12 and 200 cps in Figure 13 which closely corresponds to the reciprocal of the time lag between paths #2 and #3. The remaining two energy concentrations at 325 and 415 cps in Figure 12, and at 300 and 445 cps in Figure 13, appear to be associated with frequencies present in the first bubble collapse itself. A small energy concentration appears at 105 cps in both figures which is the reciprocal of the interval between the first and second bubble collapses as illustrated in Figure 2. Thus, there appear to be two main factors controlling the frequency spectrum of the received reflections: (1) the depths of the source and receiver and (2) the nature of the first bubble collapse which is effected by source depth, energy in the discharge, and the vagaries of the energy coupling between the source and the water.

The relationships between the energy spectrums of bottom and sub-bottom reflections in Figures 12 and 13 are very interesting. The energy from the sub-bottom reflection is often greater than that from the bottom reflection. This is easily explainable in terms of appropriately valued reflection and transmission coefficients at sedimentary interfaces. It is unexpected to find that the ratio of sub-bottom to bottom reflected energies does not steadily decrease with increasing frequency.

Since the seismic returns for Figures 12 and 13 were obtained between one and two nautical miles apart and involved the same sedimentary layer, it would be reasonable to expect the ratio of sub-bottom to bottom reflected energies to be the same in both figures at the same frequency. This is true in many cases. For example, both Figures 12 and 13 show the sub-bottom reflected energy to be greater

than the bottom reflected energy at 325 cps. On the other hand, there are frequencies such as 100 cps where such agreement does not exist. These matters will all be covered in section 3.3.3 below in terms of attenuation in the sedimentary layer.

### 3.3.3 Attenuation in the Sedimentary Layer

The acoustic attenuation in the first sedimentary layer is plotted in Figure 14 as determined from each of the two seismic returns. The most unexpected thing about the plots is that a steady increase in attenuation with increasing frequency does not appear. This is in disagreement with all of the theoretical and empirical absorption studies cited in the introduction to this monograph which were done for frequency ranges above 4 kcps. However, attenuation behavior of the kind shown in Figure 14 does appear in the empirical energy spectrum plots made by Meyer.<sup>16</sup> Meyer's plots covered the same frequency range as that investigated in this study.

Close examination of the two curves in figure 14 reveals a great deal of agreement, particularly above 300 cps. Below 300 cps agreement can also be observed but at frequencies slightly displaced from one another. Generally, both curves indicate fairly well agreeing regions of high and low attenuation.

Many of the points (plotted at 5 cps intervals) on the curves in Figure 14 were determined at very low energy levels. It was felt that at frequencies where either the energy of the bottom or sub-bottom reflection was too low, unreliability of the attenuation value might possibly result. Therefore, Figure 15 was plotted which deleted all

Figure 14

ACOUSTICAL TRANSMISSION RESPONSE OF FIRST SEDIMENTARY LAYER  
AS CALCULATED FROM TWO DIFFERENT SEISMIC RETURNS

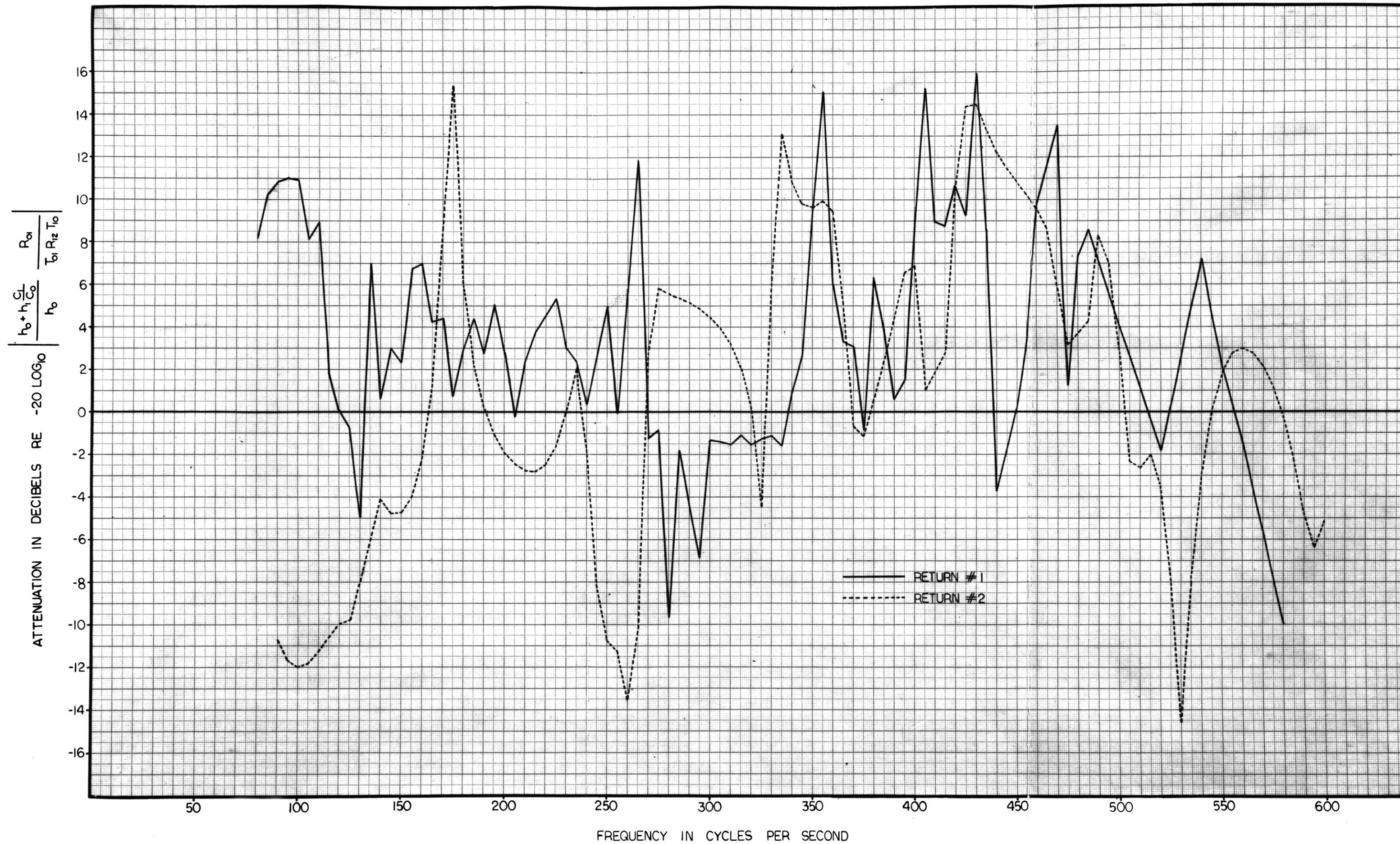


Figure 14 - ACOUSTICAL TRANSMISSION RESPONSE OF FIRST SEDIMENTARY LAYER AS CALCULATED FROM TWO DIFFERENT SEISMIC RETURNS

points where either the bottom or sub-bottom reflected energy was below 0.15 on the arbitrary scale. The smooth curves following the broad trend of the remaining points exhibit regions of high, low, high, and low attenuation in that order. Examination of some of the groupings of points shows such smoothness as to strongly suggest a real functional relationship.

A straight line was drawn through the points in Figure 15 to catch the general linear trend. The slope of this line is about 1/75 decibels per cps or 1/0.075 decibels per kcps. Using the earlier calculated 400 foot thickness of the sedimentary layer, the attenuation becomes  $1/(0.075)(800) = 1/60$  decibels per foot per kcps. This compares quite favorably with the slope of 1/50 decibels per foot per kcps determined by Wood and Weston<sup>10</sup> for the frequency range above 4 kcps.

Figure 15

ACOUSTICAL TRANSMISSION RESPONSE OF FIRST SEDIMENTARY LAYER  
AS CALCULATED FROM TWO DIFFERENT SEISMIC RETURNS

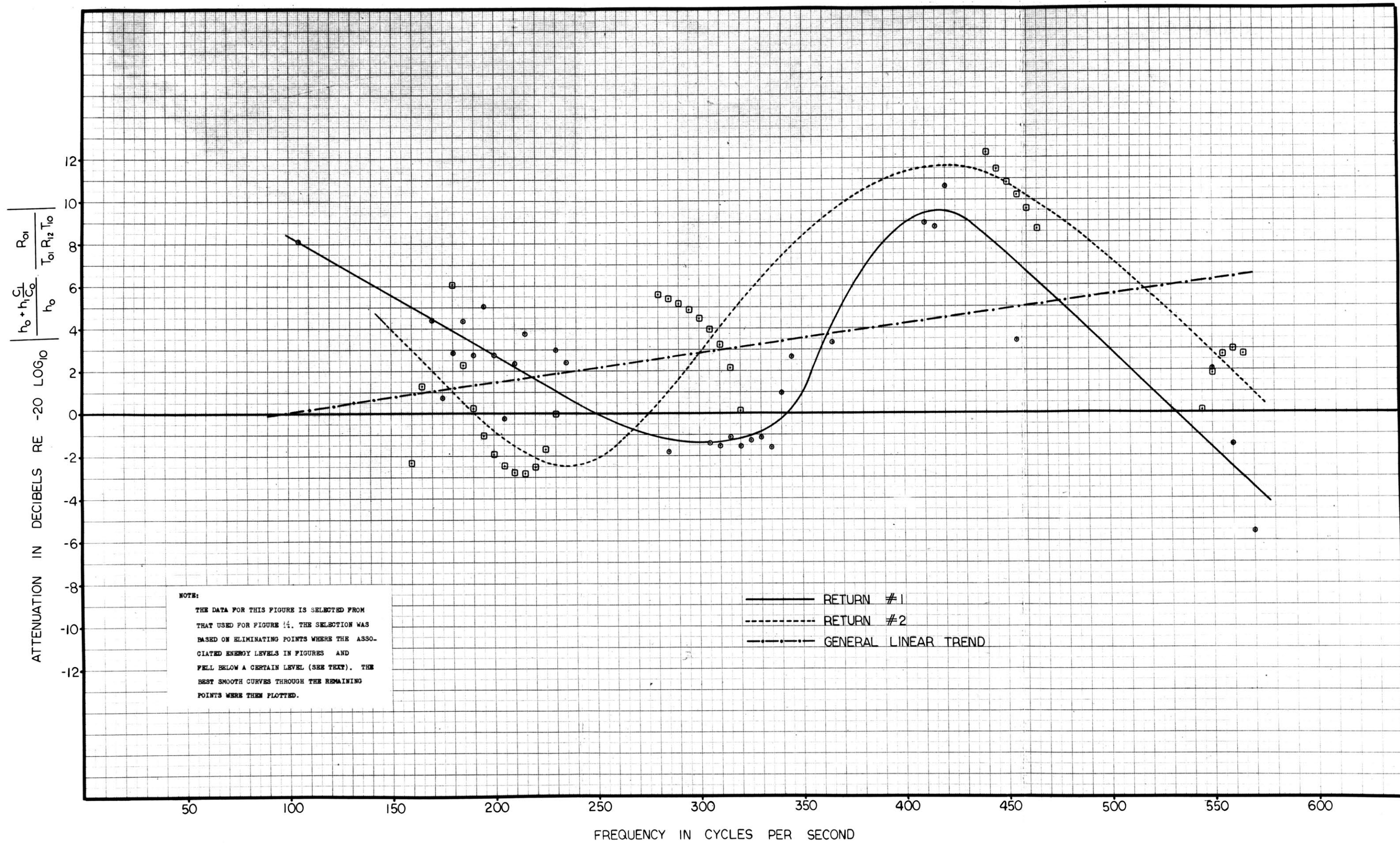


Figure 15 - ACOUSTICAL TRANSMISSION RESPONSE OF FIRST SEDIMENTARY LAYER AS CALCULATED FROM TWO DIFFERENT SEISMIC RETURNS

#### 4.0 CONCLUSIONS

This investigation has indicated that an in situ oceanic sedimentary layer exhibits an acoustical attenuation in the 75 to 600 cps frequency range which varies up and down in magnitude. The analysis reflected this both in fine detail (Figure 13) and in broad trend (Figure 14). The acoustical absorption studies of workers cited in the introduction show a steady increase in absorption with increasing frequency for ranges above 4 kcps. Extrapolation of those results down to the 75 to 600 cps frequency range appears to be in disagreement with the attenuation behavior observed in this study. On the other hand, Meyer's frequency spectrums<sup>16</sup> in the 75 to 600 cps range indicate an up and down attenuation such as was obtained by the writer. The up and down attenuation observed in this study appears to be superimposed on a linearly increasing curve whose slope closely agrees with that determined by Wood and Weston.<sup>10</sup> A considerable amount of additional data must be analyzed before the results of this study can be considered as valid.

Although the results of this study are unexpected, it may well be that they are not in disagreement with the theory and empirical results of the workers mentioned in the introduction. It must be remembered that the work of those cited in the introduction was carried out in frequency ranges considerably higher than the frequency range treated in this investigation. The disagreement mentioned earlier was based on comparing results of others extrapolated into the frequency range considered in this study. It is possible, although quite unlikely, that the theoretical and empirical work of the others if extended into the

low frequencies would have produced results similar to those reported herein.

More importantly, except for Wood and Weston,<sup>10</sup> the experiments of other workers were conducted in a laboratory. And even Wood and Weston's experiments were not at all of the same type as accomplished in this investigation. Their experiments consisted of placing both source and receiver in an in situ oceanic sediment. In other words, the experiments that were performed by the other workers did not involve the reflection and transmission of sound at sedimentary interfaces as was the case in this investigation.

It is, therefore, suspected that the surprising results of this investigation, if valid, may have something to do with the sedimentary interfaces and/or an aggregate behavior of a sedimentary layer within its geological environment. For example, it is possible that the reflection and transmission coefficients at the sedimentary interfaces are frequency dependent. Although, it does not seem that this should be the case for reasons stated earlier in this monograph. It is also possible that micro-layering exists between the main interfaces which would cause the observed effect. Another very interesting hypothesis involves the resonance vibration of the entire sedimentary layer.

Work reported by Whitman<sup>1</sup> on the analysis of foundation vibrations lends support to the last hypothesis above. Civil engineers have long known that operating machinery can excite a foundation into certain resonance vibrations. One of the very simple equations for the resonance frequency  $f_r$  of a foundation is shown in equation (20). For this equation, the foundation is considered to be a rigid mass on an elastic body.

$$(20) \quad f_r = f_n = \frac{1}{2\pi} \left[ \frac{k}{M_f + M_s} \right]^{1/2}$$

where:  $f_n \equiv$  The undamped natural frequency

$k \equiv$  The spring constant of the soil (ratio of load to movement)

$M_f \equiv$  The mass of the foundation block plus machinery

$M_s \equiv$  The equivalent mass of the soil

Whitman<sup>1</sup> discusses the difficult evaluation of  $k$  and  $M_s$  which are shown to be functions of the soil's shear modulus  $G$ , Poisson's ratio  $\mu$ , mass density  $\rho$ , and the radius of contact  $R$  between the foundation and the soil.

It may be that a situation analogous to the foundation vibration problem exists in marine seismic reflection work. Could not the first sub-bottom sedimentary layer be considered analogous to the foundation? And, could not the second sub-bottom sedimentary layer be analogous to the elastic soil medium upon which the foundation rests? If so, the attenuation of the sedimentary layer at resonance frequencies would be very high relative to surrounding frequencies. Based on limited data, this type of effect was observed in this investigation.

An immediately apparent objection to the above hypothesis is that the sedimentary layer seems too thick to be set into an aggregate resonance vibration by a seismic sound pulse of such low energy and short duration. On the other hand, perhaps resonance vibration, if it takes place at all, need not take place throughout the entire thickness of the layer at once.

If the above hypothesis is true, an extremely complicated theoretical

problem exists involving many properties of the sediments and the interrelationships among the sedimentary layers and the water. It is quite obvious that a great deal more experimental work is needed to establish the validity of the results of this investigation before the difficult theoretical approach is made.

In fine, the results of this study, if valid, are very exciting. First, they indicate that there are "windows" and "opaque" regions in the 75 to 600 cps frequency spectrum which would have obvious and important application in the design of sound sources for deep sediment penetration. Second, they indicate that a phenomenon may exist which would have application to sediment recognition using sound. That is, it could be that the shape of the attenuation plot (e.g., the location of resonance frequencies) would provide important clues as to the sediment type. And third, they indicate the possible presence of a tool which could aid in the prediction of resonance frequencies of foundations in a marine environment.

## 5.0 RECOMMENDED FUTURE INVESTIGATION

The investigation discussed in this monograph has opened areas for additional work which could possibly be of great scientific and commercial value. In view of this, some recommendations for future work are made below.

Two seismic returns were analyzed in detail in this investigation. Similar treatment of several hundred returns would provide valuable information to test the validity of the results reported herein. If such additional analysis indicated the same type of attenuation as was observed in this study, then it would be appropriate to set up a more extensive experiment such as described below to probe the causes of such acoustical behavior.

An area should be located with a horizontal sedimentary layer on the bottom having well defined interfaces. The layer should be about 200 feet thick and in water shallow enough for divers to work on the bottom. One hydrophone should be placed a number of feet above the bottom. Two more hydrophones 15 or 20 feet apart and one above the other, should be placed a number of feet below the bottom in the first sedimentary layer. A wide-band sound source capable of emitting short sound pulses relative to those of a sparker should be located near the water's surface. Perhaps two tape recorders should be employed so that the pulses received at different hydrophones could be easily separated. Correlation between pulses recorded on different tapes could easily be accomplished by counting the pulses from an experiment's start.

Quite a number of spectral comparisons of various reflected and transmitted pulses are obviously possible with the above set-up, including the type accomplished in this investigation. These would lead to the determination of the upgoing and downgoing reflection and transmission coefficients at the ocean's bottom, and the downgoing reflection coefficient at the first interface below the bottom. Additionally, it should be possible to determine the attenuation within the sedimentary layer using the two sub-bottom hydrophones. An important part of these determinations would be to learn the various parameters' dependency on frequency. A large number of reflections in one location could be analyzed to determine the repeatability of results from one sound pulse to the next.

The quiet conditions and the great flexibility of the above arrangement should allow the adequate testing of the results of this study plus a determination of the causes of the results. The next step would be to perform similar experiments in other areas to determine the effects of sediment type and thickness of the layer.

REFERENCES

- (1) Whitman, R. V., "Analysis of Faridation Vibrations," Professional Paper P65-02, Soils Publication 169, Massachusetts Institute of Technology, Cambridge, Mass., April 1964.
- (2) J. B. Hersey, "Continuous Reflection Profiling," The Sea Vol. 3 (edited by M. N. Hill), Interscience Publishers, 1963, pp. 47-72.
- (3) J. B. Hersey and M. Ewing, "Seismic Reflections from Beneath the Ocean Floor," TRANSACTIONS OF THE AMERICAN GEOPHYSICAL UNION, Vol. 30, 1949, pp. 5-14.
- (4) W. S. Ament, "Sound Propagation in Gross Mixtures," JOURNAL OF THE ACOUSTICAL SOCIETY OF AMERICA, Vol. 25, 1953, pp. 638-641.
- (5) M. A. Biot, "Theory of Propagation of Elastic Waves in a Fluid Saturated Porous Solid. I. Low Frequency Range," JOURNAL OF THE ACOUSTICAL SOCIETY OF AMERICA, Vol. 28, 1956, pp. 168-178.
- (6) M. A. Biot, "Theory of Propagation of Elastic Waves in a Fluid Saturated Porous Solid. II. Higher Frequency Range," JOURNAL OF THE ACOUSTICAL SOCIETY OF AMERICA, Vol. 28, 1956, pp. 179-191.
- (7) G. Shumway, "Sound Speed and Absorption Studies of Marine Sediments by a Resonance Method - Part I," GEOPHYSICS, Vol. XXV, No. 2, April 1960, pp. 451-467.
- (8) G. Shumway, "Sound Speed and Absorption Studies of Marine Sediments by a Resonance Method - Part II," GEOPHYSICS, Vol. XXV, No. 3, June 1960, pp. 659-682.
- (9) R. J. Urick, "The Absorption of Sound in Suspensions of Irregular Particles," JOURNAL OF THE ACOUSTICAL SOCIETY OF AMERICA, Vol. 20, 1948, pp. 115-119.
- (10) A. B. Wood and D. E. Weston, "The Propagation of Sound in Mud," ACUSTICA, Vol. 14, 1964, pp. 156-161.
- (11) W. D. Moon, "An Investigation of the Underwater Spark," (Unpublished Bachelor's thesis, The Massachusetts Institute of Technology, Cambridge, Mass.) 1958.
- (12) W. M. Ewing, W. S. Jardetzky and F. Press, Elastic Waves in Layered Media, McGraw-Hill Book Company, Inc., 1957.

- (13) C. B. Officer, Introduction to the Theory of Sound Transmission, McGraw-Hill Book Company, Inc., 1958.
- (14) J. W. Horton, Fundamentals of Sonar, United States Naval Institute, 1959.
- (15) S. J. Mason and H. J. Zimmermann, Electronic Circuits, Signals, and Systems, John Wiley & Sons, Inc., 1960.
- (16) S. G. Meyer, "Frequency Spectrums of Normal Incidence Reflections on the Bermuda Rise," (Unpublished Bachelor's thesis, The Massachusetts Institute of Technology, Cambridge, Mass.) 1964.